**Steel and Composite Structures**, *Vol. 25, No. 3 (2017) 337-346*
DOI: https://doi.org/10.12989/scs.2017.25.3.337


# Bending performance of laminated sandwich shells in hyperbolic paraboloidal form

Veysel Alankaya[*1] and Cengiz Erdönmez[2a]

[1]*Department of Naval Architecture, Turkish Naval Academy, Tuzla, 34942 Istanbul, Turkey*
[2]*Department of Mathematics, Turkish Naval Academy, Tuzla, 34942 Istanbul, Turkey*

(*Received March 29, 2017, Revised June 23, 2017, Accepted July 12, 2017*)

**Abstract.** Sandwich shells made of composite materials are the main focus on recent literature parallel to the requirements of industry. They are commonly chosen for the modern engineering applications which require moderate strength to weight ratio without dependence on conventional manufacturing techniques. The investigations on hyperbolic paraboloidal formed sandwich composite shells are limited in the literature contrary to shells that have a number of studies, consisting of doubly curved surfaces, arbitrary boundaries and laminations. Because of the lack of contributive data in the literature, the aim of this study is to present the effects of curvature on hyperbolic paraboloidal formed, layered sandwich composite surfaces that have arbitrary boundary conditions. Analytical solution methodology for the analyses of stresses and deformations is based on Third Order Shear Deformation Theory (TSDT). Double Fourier series, which are specialized for boundary discontinuity, are used to solve highly coupled linear partial differential equations. Numerical solutions showing the effects of shell geometry are presented to provide benchmark results.

**Keywords:** sandwich composites; hyperbolic paraboloidal shell; boundary-discontinuity; fourier series

## 1. Introduction

Laminated composites with their tailored properties have wide range of application area in engineering disciplines, which have the necessity of light weighted materials with high stiffness capabilities. They can be preferred for a wide range of different applications. Major reason for this decision is not only the influence of high stiffness to weight ratios for reducing weight but also the decrease in the construction cost as a result of molding complex geometries instead of machining. Therefore it is consistent to develop new materials to find the most accurate solution methodology describing the physics of detailed design and working conditions of laminated composite structures.

Hyperbolic shells are commonly used by architects for creative purposes to combine the technique and art in modern buildings. Therefore the literature is commonly consist of the studies about architectural aspects. Ortega and Robles (2003) presented a shape optimization methodology considering the effects of geometrical parameters. The behavior of hyperbolic paraboloid shaped roofs, considering the deflection of the surface caused by aerodynamic loads, is presented by Rizzo *et al.* (2011, 2012a,b, 2015).

Hyperbolic shells as being the most attractive visualization for creating new designs for architects are also new focus on aerospace and shipbuilding industry because of the integration problems arise between different surfaces with different curvatures. As an example of such surfaces, the conjunction of wings and body of an airplane or sonar dome and ship hull made of composite materials can be mentioned.

Most of the shell geometries with arbitrary laminations and boundaries can be found in the literature, but the hyperbolical forms which can be seen in the space, aviation or marine applications, are reported very recently in several studies (Ishakov 1999, Singh *et al.* 2009, Fraternali *et al.* 2014, Lachenal *et al.* 2014, Chaudhuri *et al.* 2015 a,b, Vinson 2005, Zenkour and Youssif 2000, Chen 2007). Because of the lack of contributive data in the literature, the aim of this study is to present the effects of hyperbolic paraboloidal form on the performance of the sandwich shells having one or double core layers.

## 2. Hyperbolic paraboloid surfaces

It is convenient to define and describe the hyperbolic paraboloidal surfaces before presenting its solution methodology for laminated sandwich composite material at the beginning.

Hyperbolic paraboloids, as a particular case of a doubly-curved shell which is described by principal curvature lines, are generated by moving a parabola on another one. The position vector of the hyperbolic paraboloid is given as $r(\alpha_1, \alpha_2)$ by Tornabene and Fantuzzi (2014)

*Corresponding author, Ph.D.,
E-mail: valankaya@dho.edu.tr
[a] Ph.D.
E-mail: cerdonmez@dho.edu.tr



ISSN: 1229-9367 (Print), 1598-6233 (Online)

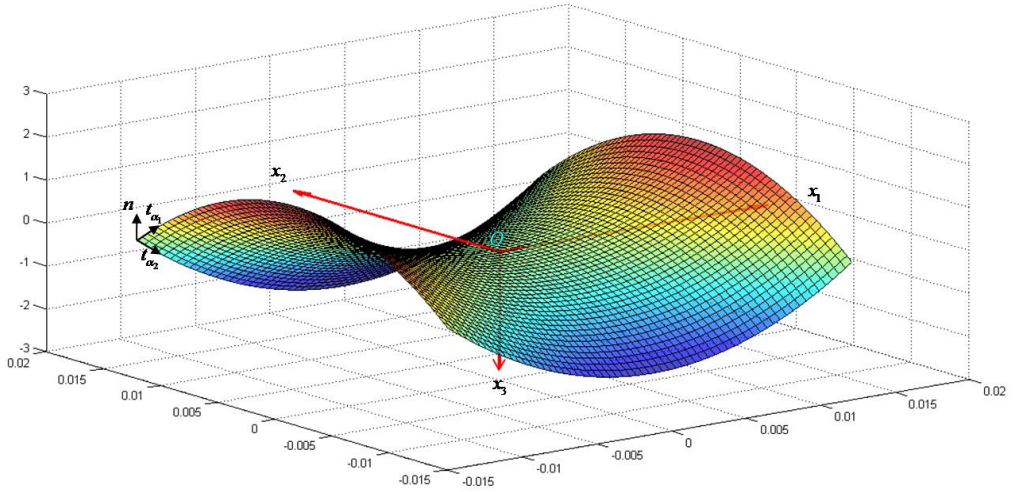


Fig. 1 The position vector $r(\alpha_1,\alpha_2)$ of the Hyperbolic Paraboloid

$$r(\alpha_1,\alpha_2)=\left(\frac{k^{\alpha_1}\tan\alpha_1}{2}+\frac{k^{\alpha_2}\tan^2\alpha_2}{4}\sin\alpha_1\right)e_1-\frac{k^{\alpha_2}\tan\alpha_2}{2}e_2+\left(\frac{k^{\alpha_1}\tan^2\alpha_1}{4}-\frac{k^{\alpha_2}\tan^2\alpha_2}{4}\cos\alpha_1\right)e_3 \quad (1)$$

where $k^{\alpha_1}$, $k^{\alpha_2}$ are the characteristic parameters of two parabolas and $\alpha_1$, $\alpha_2$ are the angles of normals with $\alpha_{1,2}\in\left[-\frac{\pi}{2},\frac{\pi}{2}\right]$. The first and second order derivatives of the position vector for hyperbolic paraboloid can be written as

$$r_{,\alpha_1}=\left(\frac{1}{2}k^{\alpha_1}(1+\tan^2\alpha_1)+\frac{1}{4}k^{\alpha_2}\tan^2\alpha_2\cos\alpha_1\right)e_1+\left(\frac{1}{2}k^{\alpha_1}\tan\alpha_1(1+\tan^2\alpha_1)+\frac{1}{4}k^{\alpha_2}\tan^2\alpha_2\sin\alpha_1\right)e_3 \quad (2)$$

$$r_{,\alpha_2}=\left(\frac{1}{2}k^{\alpha_2}\tan\alpha_2\sin\alpha_1(1+\tan^2\alpha_2)\right)e_1-\left(\frac{1}{2}k^{\alpha_2}(1+\tan^2\alpha_2)\right)e_2-\left(\frac{1}{2}k^{\alpha_2}\tan\alpha_2\cos\alpha_1(1+\tan^2\alpha_2)\right)e_3 \quad (3)$$

$$r_{,\alpha_1\alpha_1}=\left(k^{\alpha_1}\tan(\alpha_1)(1+\tan^2\alpha_1)-\frac{1}{4}k^{\alpha_2}\tan^2\alpha_2\sin\alpha_1\right)e_1+\left(\frac{1}{2}k^{\alpha_1}(1+\tan^2\alpha_1)(1+3\tan^2\alpha_1)+\frac{1}{4}k^{\alpha_2}\tan^2\alpha_2\cos\alpha_1\right)e_3 \quad (4)$$

$$r_{,\alpha_2\alpha_2}=\left(\frac{1}{2}k^{\alpha_2}(1+\tan^2\alpha_2)(1+3\tan^2\alpha_2)\sin\alpha_1\right)e_1-\left(k^{\alpha_2}\tan\alpha_2(1+\tan^2\alpha_2)\right)e_2-\left(\frac{k^{\alpha_2}}{2}\cos\alpha_1(1+\tan^2\alpha_2)(1+3\tan^2\alpha_2)\right)e_3 \quad (5)$$

$$r_{,\alpha_1\alpha_2}=\left(\frac{1}{2}k^{\alpha_2}\tan\alpha_2\cos\alpha_1(1+\tan^2\alpha_2)\right)e_1+\left(\frac{1}{2}k^{\alpha_2}\tan\alpha_2\sin\alpha_1(1+\tan^2\alpha_2)\right)e_3 \quad (6)$$

Using the relations given in Eqs. (2)-(6) the first fundamental coefficients can be written as

$$\begin{aligned}E(\alpha_1,\alpha_2)&=r_{,\alpha_1}\cdot r_{,\alpha_1}=\left(\frac{1}{2}k^{\alpha_1}(1+\tan^2\alpha_1)+\frac{1}{4}k^{\alpha_2}\tan^2\alpha_2\cos\alpha_1\right)^2\\&\quad+\left(\frac{1}{2}k^{\alpha_1}\tan\alpha_1(1+\tan^2\alpha_1)+\frac{1}{4}k^{\alpha_2}\tan^2\alpha_2\sin\alpha_1\right)^2\\F(\alpha_1,\alpha_2)&=r_{,\alpha_1}\cdot r_{,\alpha_2}=0\\G(\alpha_1,\alpha_2)&=r_{,\alpha_2}\cdot r_{,\alpha_2}=\left(\frac{1}{2}\frac{k^{\alpha_2}}{\cos^3\alpha_2}\right)^2\end{aligned} \quad (7)$$

$$n(\alpha_1,\alpha_2)=\frac{r_{,\alpha_1}\wedge r_{,\alpha_2}}{\sqrt{EG-F^2}}=(\sin\alpha_1\cos\alpha_2)e_1+(\sin\alpha_2)e_2-(\cos\alpha_1\cos\alpha_2)e_3 \quad (8)$$

$$\begin{aligned}L(\alpha_1,\alpha_2)&=-r_{,\alpha_1\alpha_1}\cdot n=\frac{1}{4}\frac{2k_{\alpha_1}\cos^2(\alpha_2)+k\alpha_2\cos^3(\alpha_1)-k\alpha_2\cos^3(\alpha_1)\cos^2(\alpha_2)}{\cos(\alpha_2)\cos^3(\alpha_1)}\\M(\alpha_1,\alpha_2)&=-r_{,\alpha_1\alpha_2}\cdot n=0\\N(\alpha_1,\alpha_2)&=-r_{,\alpha_2\alpha_2}\cdot n=-\frac{1}{2}\frac{k_{\alpha_2}}{\cos^3(\alpha_2)}\end{aligned} \quad (9)$$

Principal radii of curvatures $R_1$, $R_2$ and the Lamè parameters $A_1$, $A_2$ of the surface are given as

$$R_1=\frac{E}{L}=\frac{\frac{1}{2}\frac{k^{\alpha_1}}{\cos^3\alpha_1}+\frac{1}{4}k^{\alpha_2}\tan^2\alpha_2}{\cos\alpha_2},\quad R_2=\frac{G}{N}=-\frac{1}{2}\frac{k^{\alpha_2}}{\cos^3\alpha_2}, \quad (10)$$

$$A_1=\sqrt{E}=\frac{1}{2}\frac{k^{\alpha_1}}{\cos^3\alpha_1}+\frac{1}{4}k^{\alpha_2}\tan^2\alpha_2,\quad A_2=\sqrt{G}=\frac{1}{2}\frac{k^{\alpha_2}}{\cos^3\alpha_2}, \quad (11)$$

If the principle curvatures have different signs then it means that the Gaussian curvature is negative, because of $R_1>0$ while $R_2>0$, which characterize that the surface is a doubly-curved surfaces and named as hyperbolic shape. From Eq. (10) it can be observed that the position vector defined in Eq. (1) corresponds to a hyperbolic paraboloid. The ratio of the principal radii of curvatures for hyperbolic paraboloidal surface can be defined by $\frac{R_1}{R_2}$ as

$$\frac{R_1}{R_2}=-\left(\frac{\sin^2\alpha_2}{2}+d\frac{\cos^2\alpha_2}{\cos^3\alpha_1}\right) \quad (12)$$

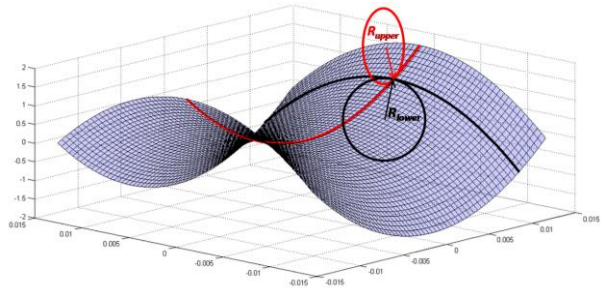


Fig. 2 Hyperbolic paraboloid surface and radius of upper and lower parabolas

where $d$ is defined by the ratio of characteristic parameters of two parabolas as, $d = \frac{k^{\alpha_1}}{k^{\alpha_2}}$. The position vector $r(\alpha_1, \alpha_2)$, described in Eq. (1), of the hyperbolic paraboloid is illustrated in Fig. 1.

If we determine a curvature parameter $(\Im)$ considering the respect ratio of the radiuses of upper ($R_1$) and lower ($R_2$) parabolas $\left(\Im = {R_{upper}}/{R_{lower}}\right)$, it will have negative sign $(\Im < 0)$ because one of the parabolas has the radius in reverse orientation by centered in negative -*z*- axis, as presented in Fig. 2. Radiuses of osculating circles at intersection point of selected surface parabolas are plotted for illustration purposes in Fig. 2. Since the surface has double curvature at predefined intersection point, the surface having two radiuses as upper and lower parabolas can be examined by the theories developed for doubly curved shells.

## 3. Analyzing the doubly curved composite shells using TSDT

Since some of the in-plane and plate stiffness properties are dominated by the transverse shear deformations, their effects are important for laminated composite structures. Therefore, for polymer matrix laminated composite plates, transverse shear deformation effects can be significant. However they have been neglected in classical plate theories (Khalili *et al.* 2012). This assumption causes the theory to be inadequate for modeling composite plates, even if the plate is fairly thin. The first order shear deformation plate theory yields a constant value of transverse shearing strain through the thickness of the plate, and thus requires shear correction factors to ensure the proper amount of transverse shear energy (Viola *et al.* 2013). The reliable prediction of deformations and stresses especially for the thicker structures requires the use of higher order shear deformation theories (Viola *et al.* 2013).

Development of various new higher order deformation theories is continuous with consistent effort. The increasing use of laminated shell structures in engineering applications requires adequate instruments in order to achieve refined solutions to the shell problems under investigation. Therefore a significant number of higher order shear deformation theories for composite plates and shells has been presented over the last decades (Alankaya and Oktem 2016, Mantari *et al.* 2012a,b,c,d, Zenkour 2013, Zhen and Wanji 2007, Ferreira *et al.* 2003, Reddy 2003, Youssif 2009). It has valuable importance to indicate that Zhen and Wanji (2007) studied higher order theories to ninth-order and presented the higher order components resulted in the higher accuracy of transverse shear stresses. However, they reported that the results obtained by the ninth-order theory had almost negligible differences. In principle, it is possible to expand the displacement field in terms of the thickness coordinate up to any desired degree. However, due to the algebraic complexity and computational effort requirements with higher order theories contrary for marginal gain in accuracy, theories for higher than third order, have not been attempted (Zhen and Wanji 2007).

The third-order assumption in the displacement field satisfies the continuity conditions of transverse shear stresses at the layer interfaces as well as the conditions of zero transverse shear stresses on the plate boundary surface fulfilling the need of shear correction factor. Thus TSDT eliminates the need to compute shear correction factors, which is a requirement for the first order shear deformation theory (FSDT). TSDT of Reddy is based on the same assumptions as the classical and first-order theories except that the assumption of straightness and normality of a transverse normal after deformation is relaxed by expanding the displacements as cubic functions of the thickness coordinate. In addition it is subject to the following assumptions and restrictions (Reddy 2003): *(i)* The layers are perfectly bonded together, *(ii)* The material of each layer is linearly elastic and has three planes of material symmetry (orthotropic), *(iii)* Each layer is of uniform thickness, *(iv)* The strains and displacements are small, *(v)* The transverse shear stresses on top and bottom surfaces of the laminate are zero.

Since it represents the kinematics better while disregarding shear correction factor and yields more accurate transverse shear stresses with minimum computational effort, Third Order Shear Deformation Theory (TSDT) of Reddy (2003) is preferred for the analyses of laminated composite shell for this study. Because of its simplicity and proven accuracy among other higher order theories that are present in the literature.

## 4. Definition of the problem

$$u_1 = u(\xi_1,\xi_2,\xi_3) = u_0(\xi_1,\xi_2) + z\phi_1(\xi_1,\xi_2) - \frac{4}{3h^2}z^3\left(\phi_1 + \frac{\partial w_0}{\partial \xi_1}\right)$$
$$u_2 = v(\xi_1,\xi_2,\xi_3) = v_0(\xi_1,\xi_2) + z\phi_2(\xi_1,\xi_2) - \frac{4}{3h^2}z^3\left(\phi_2 + \frac{\partial w_0}{\partial \xi_2}\right) \quad (13)$$
$$u_3 = w(\xi_1,\xi_2,\xi_3) = w_0(\xi_1,\xi_2)$$

where *u, v, w* represents displacements of a point at three axis $(\xi_1, \xi_2, \xi_3)$, while $u_0, v_0, w_0$ represents displacements of a point at the mid-surface $(\xi_3 = 0)$. $\phi_1$ and $\phi_2$ are rotations about $(\xi_2)$ and $(\xi_1)$ axes respectively.

The equations obtained by using the principles of virtual work and constitutive relations for composite materials are presented extensively in Appendix-A. The set of five highly coupled fourth-order partial differential equations can be expressed in the following matrix form

$$\left[K_{ij}\right]\left\{X_j\right\}=\left\{f_i\right\} \text{ which } (i,j=1,...,5) \text{ and } (K_{ij}=K_{ji}) \tag{14a}$$

where

$$\{x_j\}^T=\{u_1 \;\; u_2 \;\; u_3 \;\; \phi_1 \;\; \phi_2\} \tag{14b}$$

$$\{f_i\}^T=\{0 \;\; 0 \;\; -Q_{mn} \;\; 0 \;\; 0\} \tag{14c}$$

The definitions of $[K_{ij}]$ coefficient matrix are given in Appendix-B and the load term $Q_{mn}$ is defined as follow

$$Q_{mn}=\frac{16q}{\pi^2 mn} \tag{15}$$

for uniformly distributed load where *m,n* are the number of terms. The problem considered in this study is solved for the following boundary conditions; The simply supported type 1 (*SS1*) boundary conditions are prescribed at the edges $\varsigma_1=0,a$.

$$N_1=N_6=u_3=M_1=P_1=\phi_2=0 \tag{16a}$$

and the simply supported type 4 (*SS4*) boundary conditions prescribed at the edges $\varsigma_2=0,b$.

$$u_1=u_2=u_3=M_2=P_2=\phi_1=0 \tag{16b}$$

## 5. Solution methodology

$$\begin{aligned}
u_1(\xi_1,\xi_2)&=\sum_{m=0}^{\infty}\sum_{n=1}^{\infty}U_{mn}\Re_1(\xi_1,\xi_2) && 0\le\xi_1\le a \quad 0\le\xi_2\le b\\
u_2(\xi_1,\xi_2)&=\sum_{m=1}^{\infty}\sum_{n=0}^{\infty}V_{mn}\Re_2(\xi_1,\xi_2) && 0<\xi_1<a \quad 0<\xi_2<b\\
u_3(\xi_1,\xi_2)&=\sum_{m=1}^{\infty}\sum_{n=1}^{\infty}W_{mn}\Re_3(\xi_1,\xi_2) && 0\le\xi_1\le a \quad 0\le\xi_2\le b\\
\phi_1(\xi_1,\xi_2)&=\sum_{m=0}^{\infty}\sum_{n=1}^{\infty}X_{mn}\Re_1(\xi_1,\xi_2) && 0\le\xi_1\le a \quad 0\le\xi_2\le b\\
\phi_2(\xi_1,\xi_2)&=\sum_{m=1}^{\infty}\sum_{n=0}^{\infty}Y_{mn}\Re_2(\xi_1,\xi_2) && 0\le\xi_1\le a \quad 0\le\xi_2\le b
\end{aligned} \tag{17}$$

where

$$\begin{aligned}
\Re_1(\xi_1,\xi_2)&=\cos(\alpha\xi_1)\sin(\beta\xi_2),\\
\Re_2(\xi_1,\xi_2)&=\sin(\alpha\xi_1)\cos(\beta\xi_2),\\
\Re_3(\xi_1,\xi_2)&=\sin(\alpha\xi_1)\sin(\beta\xi_2),
\end{aligned} \tag{18}$$

$$\alpha=\frac{m\pi}{a},\quad \beta=\frac{n\pi}{b}$$

The next step is substituting assumed particular solutions into equilibrium equations. The procedure for differentiation of these functions is based on Lebesque integration theory which introduces boundary Fourier coefficients arising from discontinuities of the particular solutions at the edges. Chaudhuri (2002) has been noted that the boundary Fourier coefficients serve as complementary solution to the considered problem. The partial derivatives which cannot be obtained by term wise differentiation, for the considered boundary conditions, are given by (Oktem *et al.* 2013) as follows

$$\begin{aligned}
u_{2,1}=&\frac{1}{4}\bar{a}_0+\frac{1}{2}\sum_{n=1}^{\infty}\bar{a}_n\cos(\beta\varsigma_2)+\frac{1}{2}\sum_{m=1}^{\infty}\left[\alpha V_{m0}+\gamma_m\bar{a}_0+\psi_m\bar{b}_0\right]\cos(\alpha\varsigma_1)\\
&+\sum_{m=1}^{\infty}\sum_{n=1}^{\infty}\left[\alpha V_{mn}+\gamma_m\bar{a}_n+\psi_m\bar{b}_n\right]\cos(\alpha\varsigma_1)\cos(\beta\varsigma_2)
\end{aligned} \tag{19}$$

$$u_{2,2}=-\sum_{m=1}^{\infty}\sum_{n=1}^{\infty}\beta V_{mn}\sin(\alpha\varsigma_1)\sin(\beta\varsigma_2) \tag{20}$$

$$u_{2,22}=\frac{1}{2}\sum_{m=1}^{\infty}\bar{c}_m\sin(\alpha\varsigma_1)+\sum_{m=1}^{\infty}\sum_{n=1}^{\infty}\left[-\beta^2V_{mn}+\gamma_n\bar{c}_m+\psi_n\bar{d}_m\right]\sin(\alpha\varsigma_1)\cos(\beta\varsigma_2) \tag{21}$$

in which

$$(\gamma_n,\psi_n)=\begin{cases}(0,1), & n=odd,\\ (1,0), & n=even.\end{cases} \tag{22}$$

The unknown boundary Fourier coefficients appear in Eqs. (19)-(21) are defined as follows

$$\bar{a}_n,\bar{b}_n=\frac{4}{ab}\int_0^b[u_2(a,\varsigma_2)\mp u_2(0,\varsigma_2)]\cos(\beta\varsigma_2)d\varsigma_2 \tag{23}$$

$$\bar{c}_m,\bar{d}_m=\frac{4}{ab}\int_0^a[u_{2,2}(\varsigma_1,b)\mp u_{2,2}(\varsigma_1,0)]\sin(\alpha\varsigma_1)d\varsigma_1 \tag{24}$$

The remaining partial derivatives can be obtained by term wise differentiation. Solution methodology requires solution of the Fourier coefficients by using natural and geometrical boundary conditions which are presented by (Oktem *et al.* 2013) in detail and will not be repeated here for the brevity of the presentation.

## 6. Numerical results and discussions

A generic model for laminated composite shell made of structural foam core and unidirectional pre-impregnated carbon face layers are modeled for numerical analyses. The materials are commercially available and suitable for structural usage due to their high strength properties are randomly chosen from product family catalogue of Gurit AG (http://www.gurit.com). The material properties used for the face sheets and core layers in the analyses are presented in Table 1.

During the calculations, the following normalized quantities are defined and used in which '*a*' and '*b*' are the edge lengths of the hyperbolic paraboloidal shell, and $q_0$ denotes the transverse load. The normalized quantities are computed at the center of the panel and presented in figures for all numerical results.

$$u_3^*=(10^3Eh^3/q_0a^4)u_3 \tag{25a}$$

$$M_1^*=(10^3/q_0a^2)M_1 \tag{25b}$$

$$\sigma_1^*=10(h^2/q_0b^2)\sigma_1 \tag{25c}$$

$$\sigma_2^*=10(h^2/q_0b^2)\sigma_2 \tag{25d}$$

Table 1 Material properties of the face sheets and the core layer

| Part | Material | Property | |
|---|---|---|---|
| Face Sheets | Gurit® SC 110T2 (Visual Carbon Prepreg) | $0^o$ Tensile Modulus | : 69 GPa |
| | | $90^o$ Tensile Modulus | : 72 GPa |
| | | In-plane Shear Modulus | : 5 GPa |
| | | Flexural Modulus | : 60 GPa |
| Core | Gurit® Corecell™ A (Structural Foam Core A500) | Tensile Modulus | : 84 MPa |
| | | Shear Modulus | : 32 MPa |

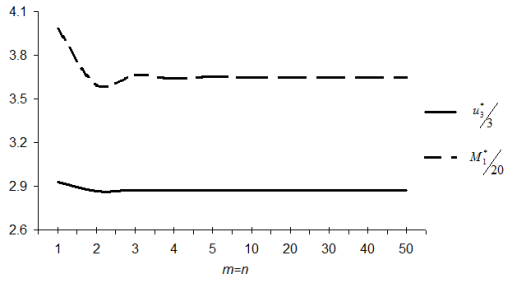


Fig. 4 Convergence of the normalized central deflection $(u_3^*)$ and moment $(M_1^*)$ for symmetrically laminated sandwich shell $[0^o/90^o/\text{core}/90^o/0^o]$

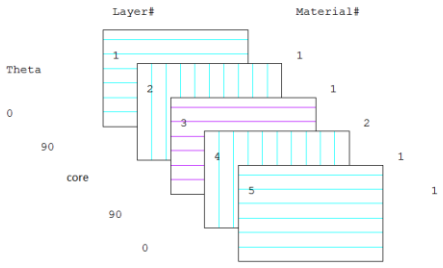


Fig. 5 Layer definitions for the Shell 91 element

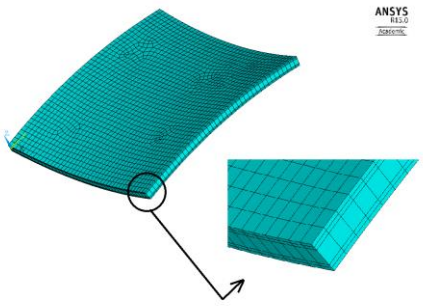


Fig. 6 The element description for the FEA model

Number of terms *(m=n)* to be included in the equations are controlled by the convergence of the solution methodology. Convergence control is performed for the symmetrically laminated sandwich shell $[0^o/90^o/\text{core}/90^o/0^o]$ having moderately thick *(a/h=10)* cross-ply face sheets and one core layer *(c/h=10)* under uniformly distributed load of 100 MPa.

Fig. 4 displays the convergence of normalized central transverse displacement $(u_3^*)$ and moment $(M_1^*)$ of a hyperbolic paraboloidal shell which has negative ratio $(\Im = -1)$ at the same radiuses of lower and upper parabolas. Normalized values $\left(u_3^*/3\,,\ M_1^*/20\right)$ are presented in Fig.4 respectively for the purpose of providing a clear view for the convergence.

The normalized displacement $(u_3^*)$ and moment $(M_1^*)$ values exhibit a fast convergence where as more than 20 terms are included in the expansion of double Fourier series. Consequently, number of terms included are defined as *n=m=20* for numerical results.

### *6.1 Validation of the presented solution*

Finite element analyses are performed by a commercially available FEA software ANSYS™ for the validation of the presented solution methodology. Hyperbolic paraboloidal shell, which has negative ratio $(\Im = -1)$ at the same radiuses of lower and upper parabolas $(R_1 = -R_2)$, is modeled with a symmetric $[0^o/90^o/\text{core}/90^o/0^o]$ lay-up. Laminate properties are defined by specifying individual layer properties as presented in Fig. 5.

The present study is mainly focused on the effects of shear deformations which are more efficient in the thick and moderately thick regime. Therefore, Shell-91 element is used which is developed for modeling thick sandwich structures and layered applications of structural shells.

Shell-91 element type with 8 nodes and six degree of freedom is suitable for nonlinear layered structural shell analyses with sandwich option. Because the chosen element type is considered for comparison purposes on meso-scale level, each ply is modeled and analyzed having one element per ply as presented in the Fig. 6.

For the validation of presented theory, a sandwich hyperbolic paraboloidal shell which has negative ratio $(\Im = -1)$ is modeled with one core layer at varying sheet *(a/h)* and core *(c/h)* thickness ratios. Central deflections under uniformly distributed load of 100 MPa are presented in Table 2 with their FEA counterparts.

For the validation of presented theory, a sandwich hyperbolic paraboloidal shell which has negative ratio $(\Im = -1)$ is modeled with one core layer at varying sheet *(a/h)* and core *(c/h)* thickness ratios. Central deflections

Table 2 Comparison of the central deflections obtained from presented theory with their FEA counterparts

| *a/h* | *c/h* | Deflection (mm) | |
|---|---|---|---|
| | | **Presented heory** | **FEA** |
| **10** | **10** | 0.000209 | 0.000223 |
| **50** | **10** | 0.001510 | 0.001457 |
| **50** | **50** | 0.025673 | 0.029325 |

under uniformly distributed load of 100 MPa are presented in Table 2 with their FEA counterparts.

The numerical results of the presented theory are in concordance with FEA counterparts and indicate that is adequately sensitive on thickness changes of both face sheets and core layer.

### *6.2 Numerical results*

Since the aim of this study is to investigate the effect of curvature on hyperbolic paraboloidal formed shells, made of sandwich composite material, numerical results are presented in figures depending on the curvature ratio $(\Im)$.

Normalized central deflections of laminated shell are presented in the Figs. 7 and 8 having one $[0^o/90^o/\text{core}/90^o/0^o]$ and double $[0^o/90^o/\text{core}/90^o/0^o]_{\text{sym}}$ core layers respectively. The effect of face sheet and core layer thicknesses at moderately thick and very thin regimes are presented regarding to the non-dimensional curvature ratio ( $\Im$ ). Moreover the effect of face sheet thickness is investigated depending on the core thickness changes and presented in Fig. 9.

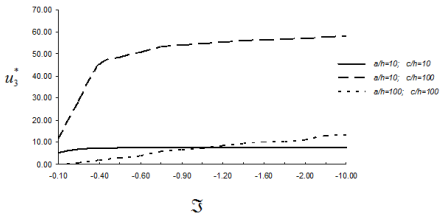


Fig. 7 Normalized central deflections for the sandwich shell having one core layer

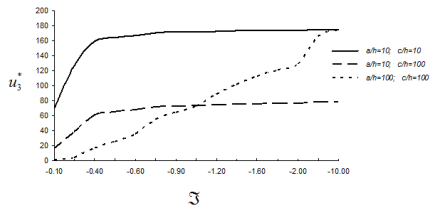


Fig. 8 Normalized central deflections for the sandwich shell having double core layer

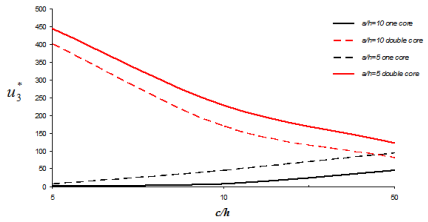


Fig. 9 Effect of thickness on the normalized central deflections

Normalized moments are presented in the Figs. 10 and 11 representing the effect of face sheet and core layer thicknesses regarding to the non-dimensional curvature ratio ( $\Im$ ). In addition, the effect of face sheet thickness is investigated depending on the core thickness changes and presented in Fig. 12.

The effects of change in face sheet and core layer thicknesses are investigated by means of stress distribution through the lamina. Normalized stress distribution through the laminated layers is presented in the Figs. 13 and 14 at varying thicknesses of one and double core layers respectively.

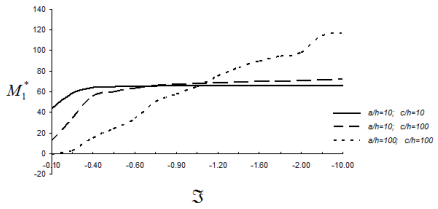


Fig. 10 Normalized moments for the sandwich shell having one core layer

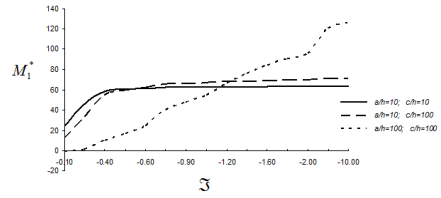


Fig. 11 Normalized moments for the sandwich shell having double core layer

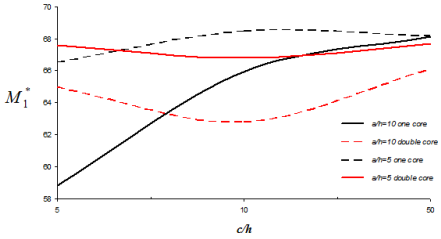


Fig. 12 Effect of thickness on the normalized moments

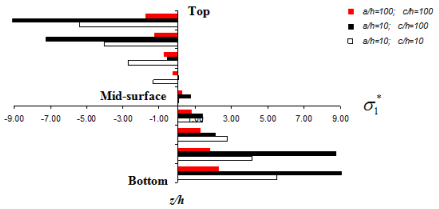


Fig. 13 Normalized stress distribution for the sandwich shell having one core layer

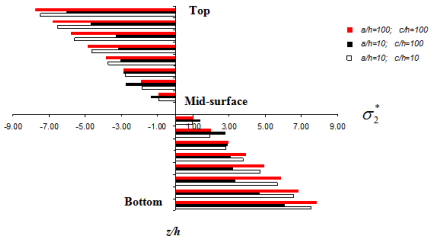


Fig. 14 Normalized stress distribution for the sandwich shell having double core layer

### *6.3 Discussion*

It is observed that the deformation behavior of the hyperbolic paraboloidal shaped laminated composite shell is affected positively by the addition of core layer as presented in Figs.7 and 8. However the rapid change in the deflection curve of the one which is in the very thin regime (*a/h=100* and *c/h=100*) is remarkable. This behavior is considered as the membrane effect which makes the shell to be stiffer at the higher curvature ratios by the addition of second core layer. Contrary to expectations the effect of curvature ratio is slightly visible for the values over $\Im > -0.5$. Therefore the effect of core thickness is investigated and presented in Fig. 9 through the changes of core layer thickness. Since the thickness of core layer causes the shell to be stiffer, its effects are considerable on the moment values and presented in Figs. 10 and 11. The change in the normalized moment through the core layer thickness is presented in Fig. 12 representing the negative effect of the second core layer addition.

The distribution through the shell thickness of normalized stress $\left(\sigma_1^*, \sigma_2^*\right)$ values are presented in Figs. 13 and 14 at varying face sheet and core layer thicknesses of the shell having one and double core layers respectively. The effect of core layer addition by means of stress values is investigated for symmetric [0°/90°/core/90°/0°] shell ($\Im$=-*1*) having one core layer and $[0^o/90^o/\text{core}/90^o/0^o]_{\text{sym}}$ shell having two core layers. While normalized stress values reach their maximum value at the top and bottom surfaces, the effect of core material thickness and additional core layer is observed as higher stress values.

## 7. Conclusions

The effect of curvature on hyperbolic paraboloidal formed sandwich composite surface having arbitrary boundary conditions is investigated by analytical methodology based on TSDT. Solution methodology based on boundary discontinuous generalized double Fourier series approach is developed for sandwich laminates having one and double core layers. Because of the lack of contributive data in the literature, numerical solutions showing the effects of shell geometry are presented to provide benchmark results. Further results are concluded as follows;

- The comparison of the results by FEA solutions that shows the predictive capabilities of the present developed methodology can be preferred for its minimized computational effort,
- Whereas extremely small deformations are obtained by the addition of second core layer, this kind of construction results decrease in stress values noticeably,
- Curvature ratio ($\Im$) values especially bigger than -0.5 has slightly visible effects on the deformation characteristics of the shell,
- Main differences on the central deflection and moment distributions are mostly effected by the changes in the thicknesses of face sheets and core layers.

To ensure the practicality and feasibility of this solution methodology, further studies are necessary to evaluate the influence of geometrical and material properties based on the deflection and stress distribution capabilities of laminated composites. While the presented methodology is not suitable for dynamic behavior of sandwich shells which can be dealt with zig-zag functions included into the kinematic model, further studies are also necessary for the dynamic capabilities of this solution methodology that should be validated by 3D finite element analyses.

## References

Alankaya, V. and Oktem, A.S. (2016), "Static analysis of laminated and sandwich composite doubly-curved shallow shells", *Steel Compos. Struct.*, **20**(5), 1043-1066.

Chaudhuri, R.A. (2002), "On the roles of complementary and admissible boundary constraints in fourier solutions to boundary-value problems of completely coupled r$^{th}$ order p.d.e.'s", *J. Sound Vib.*, **251**(2), 261-313.

Chaudhuri, R.A., Oktem, A.S. and Soares, C.G. (2015a), "Levy type boundary fourier analysis of thick cross ply panels with negative gaussian curvature", *AIAA J.*, **53**(9), 2492-2503.

Chaudhuri, R.A., Oktem, A.S. and Soares, C.G. (2015b), "Levy type boundary fourier analysis of thick clamped hyperbolic paraboloidal cross ply panels", *AIAA J.*, **53**(1), 140-149.

Chen, C.S. (2007), "The nonlinear vibration of an initially stressed laminated plate", *Composites:PartB*, **38**(4), 437-447.

Ferreira, A.J.M., Roque, C.M.C. and Martins, P.A.L.S. (2003), "Analysis of composite plates using higher-order shear deformation theory and finite point formulation based on multiquadric radial basis function method", *Composites:Part B*, **34**(7), 627-636.

Fraternali, F., Farina, I. and Carpentieri, G. (2014), "A discrete to continuum approach to the curves of membrane networks and parametric surfaces", *Mech. Res. Commun.*, **56**, 18-25.

Ishakov, V.I. (1999), "Stability analysis of viscoelastic thin shallow hyperbolic paraboloid shells", *Int. J. Solids Struct.*, **36**(28), 4209-4223.

Khalili, S.M.R., Davar, A. and Fard, K.M. (2012), "Free vibration analysis of homogeneous isotropic circular cylindrical shells based on a new three-dimensional refined higher order theory", *Int. J. Mech. Sci.*, **56**(1), 1-25.

Lachenal, X., Weaver, P.M. and Daynes, S. (2014), "Influence of transverse curvature on the stability of pre-stressed helical structures", *Int. J. Solids Struct.*, **51**(13), 2479-2490.

Mantari, J.L., Oktem, A.S. and Soares, C.G. (2012a), "A new trigonometric shear deformation theory for isotropic, laminated composite and sandwich plates", *Int. J. Solids Struct.*, **49**(1), 43-53.

Mantari, J.L., Oktem, A.S. and Soares, C.G. (2012b), "Bending and free vibration analysis of ısotropic and multilayered plates and shells by using a new accurate higher-order shear deformation theory", *Composites: Part B*, **43**(8), 3348-3360.

Mantari, J.L., Oktem, A.S. and Soares, C.G. (2012c), "Bending response of functionally graded plates by using a new higher order shear deformation theory", *Compos. Struct.*, **94**(2), 714-723.

Mantari, J.L., Oktem, A.S. and Soares, C.G. (2012d), "A new trigonometric layerwise shear deformation theory for the finite element analysis of composite and sandwich plates", *Comput. Struct.*, **94-95**, 43-53.

Oktem A.S., Alankaya, V. and Soares, C.G. (2013), "Boundary discontinuous fourier analysis of simply supported cross-ply plates", *Appl. Math. Model.*, **37**(3), 1378-1389.

Ortega, N.F. and Robles, S.I., (2003), "The design of hyperbolic paraboloids on the basis of their mechanical behaviour", *Thin Walled Struct.*, **41**(8), 769-784.

Reddy, J.N. (2003), Mechanics of Laminated Composite Plates and Shells: Theory and Analysis, second ed., CRC Press, Boca Raton, FL, USA.

Rizzo, F. (2012), "Wind tunnel tests on hyperbolic paraboloidal roofs with elliptical plane shapes", *Eng. Struct.*, **45**, 536-558.

Rizzo, F. and Sepe, V. (2015), "Static loads to simulate dynamic effects of wind on hyperbolic paraboloid roofs with square plan", *J. Wind Eng. Ind. Aerod.*, **137,** 46-57.

Rizzo, F., D'Asdia, P., Lazzari, M. and Procino, L. (2011), "Wind action evaluation on tension roofs of hyperbolic paraboloidal shape", *Eng. Struct.*, **33**(2), 445-461.

Rizzo, F., D'Asdia, P., Ricciardelli, F. and Bartoni, G. (2012), "Characterisation of pressure coefficients on hyperbolic paraboloid roofs", *J. Wind Eng. Ind. Aerod.*, **102**, 61-71.

Singh, S., Patel, B.P. and Nath, Y. (2009), "Postbuckling of angle-ply laminated cylindrical shells with meridional curvature", *Thin Walled Struct.*, **47**(3), 359-364.

Tornabene, F. and Fantuzzi, N. (2014), Mechanics of Laminated Composite Doubly-Curvel Shell Structures: The Generalized Differential Quadrature Method And The Strong Formulation Finite Element Method, Società Editrice Esculapio, Bologna.

Vinson, J.R. (2005), Plate and Panel Structures of Isotropic, Composite And Piezoelectric Materials, Including Sandwich Construction, Springer, Netherlands.

Viola, E., Tornabene, F. and Fantuzzi, N. (2013a), "Static analysis of completely doubly-curved laminated shells and panels using general higher-order shear deformation theories", *Compos. Struct.*, **101**, 59-93.

Viola, E., Tornabene, F. and Fantuzzi, N. (2013b), "General higher-order shear deformation theories for the free vibration analysis of completely doubly-curved laminated shells and panels", *Compos. Struct.*, **95**, 639-666.

Youssif, Y.G. (2009), "Non-linear design and control optimization of composite laminated doubly curved shell", *Compos. Struct.*, **88**(3), 468-480.

Zenkour, A.M. (2013), "A simple four-unknown refined theory for bending analysis of functionally graded plates", *Appl. Math. Model.*, **37**(20-21), 9041-9051.

Zenkour, A.M. and Youssif, Y.G. (2000), "Free vibration analysis of symmetric cross-ply laminated elastic plates", *Mech. Res. Commun.*, **27**(2), 65-172.

Zhen, W. and Wanji, C. (2007), "A study of global-local higher order theories for laminated composite plates", *Compos. Struct.*, **79**(1), 44-54.

*CC*

## Appendix-A. Equilibrium Equations

The equilibrium equations, which are derived using the principles of virtual work are given as follows (Reddy, 2003)

$$\frac{\partial N_1}{\partial \xi_1}+\frac{\partial N_6}{\partial \xi_2}=0 \tag{A1}$$

$$\frac{\partial N_6}{\partial \xi_1}+\frac{\partial N_2}{\partial \xi_2}=0 \tag{A2}$$

$$\frac{\partial Q_1}{\partial \xi_1}+\frac{\partial Q_2}{\partial \xi_2}-\frac{4}{h^2}\left(\frac{\partial K_1}{\partial \xi_1}+\frac{\partial K_2}{\partial \xi_2}\right)+\frac{4}{3h^2}\left(\frac{\partial^2 P_1}{\partial \xi_1^2}+\frac{\partial^2 P_2}{\partial \xi_2^2}+2\frac{\partial^2 P_6}{\partial \xi_1 \partial \xi_2}\right)=-q \tag{A3}$$

$$\frac{\partial M_1}{\partial \xi_1}+\frac{\partial M_6}{\partial \xi_2}-Q_1+\frac{4}{h^2}K_1-\frac{4}{3h^2}\left(\frac{\partial P_1}{\partial \xi_1}+\frac{\partial P_6}{\partial \xi_2}\right)=0 \tag{A4}$$

$$\frac{\partial M_6}{\partial \xi_1}+\frac{\partial M_2}{\partial \xi_2}-Q_2+\frac{4}{h^2}K_2-\frac{4}{3h^2}\left(\frac{\partial P_6}{\partial \xi_1}+\frac{\partial P_2}{\partial \xi_2}\right)=0 \tag{A5}$$

In Eqs. (A-1) to (A-5), $q$ represents the transverse load and $N_i$, $M_i$, $P_i$ *(i=1,2,6)* denotes stress resultants, stress couples and second stress couples (see, e.g., Reddy 2003). $Q_i$, *(i = 1, 2)* represents the transverse shear stress resultants given as follows

$$N_i=A_{ij}\varepsilon_j^0+B_{ij}\kappa_j^0+E_{ij}\kappa_j^2, \quad (i,j=1,2,6) \tag{A6}$$

$$M_i=B_{ij}\varepsilon_j^0+D_{ij}\kappa_j^0+F_{ij}\kappa_j^2 \tag{A7}$$

$$P_i=E_{ij}\varepsilon_j^0+F_{ij}\kappa_j^0+H_{ij}\kappa_j^2 \tag{A8}$$

$$Q_1=A_{5j}\varepsilon_j^0+D_{5j}\kappa_j^1 \quad (j=4,5) \tag{A9}$$

$$Q_2=A_{4j}\varepsilon_j^0+D_{4j}\kappa_j^1 \tag{A10}$$

$$K_1=D_{5j}\varepsilon_j^0+F_{5j}\kappa_j^1 \tag{A11}$$

$$K_2=D_{4j}\varepsilon_j^0+F_{4j}\kappa_j^1 \tag{A12}$$

in which $A_{ij}$, $B_{ij}$, etc. are the laminate rigidities (integrated stiffnesses) and defined as

$$(A_{ij},B_{ij},D_{ij})=\sum_{k=1}^{N}\int_{\xi_{k-1}}^{\xi_k}Q_{ij}^{(k)}(1,z,z^2)dz \tag{A13}$$

$$(E_{ij},F_{ij},H_{ij})=\sum_{k=1}^{N}\int_{\xi_{k-1}}^{\xi_k}Q_{ij}^{(k)}(z^3,z^4,z^6)dz \tag{A14}$$

Generalized stress – strain constitutive relations for an orthogonal lamina can be expressed as

$$\begin{Bmatrix}\sigma_1\\ \sigma_2\\ \sigma_6\\ \sigma_5\\ \sigma_4\end{Bmatrix}=\begin{bmatrix}Q_{11} & Q_{12} & 0 & 0 & 0\\ Q_{12} & Q_{22} & 0 & 0 & 0\\ 0 & 0 & Q_{66} & 0 & 0\\ 0 & 0 & 0 & Q_{55} & 0\\ 0 & 0 & 0 & 0 & Q_{44}\end{bmatrix}\begin{Bmatrix}\varepsilon_1\\ \varepsilon_2\\ \varepsilon_6\\ \varepsilon_5\\ \varepsilon_4\end{Bmatrix} \tag{A15}$$

in which ($\sigma_1$, $\sigma_2$, $\sigma_6$, $\sigma_5$, $\sigma_4$) and ($\varepsilon_1$, $\varepsilon_2$, $\varepsilon_6$, $\varepsilon_5$, $\varepsilon_4$) are the stress and strain components respectively. $Q_{ij}$ expressions in terms of engineering constants are given below

$$Q_{11}=\frac{E_1}{1-\nu_{12}\nu_{21}} \qquad Q_{44}=G_{23} \tag{A16a,b}$$

$$Q_{12}=\frac{\nu_{12}E_2}{1-\nu_{12}\nu_{21}} \qquad Q_{55}=G_{13} \tag{A17a,b}$$

$$Q_{22}=\frac{E_2}{1-\nu_{12}\nu_{21}} \qquad Q_{66}=G_{12} \tag{A18a,b}$$

$E_1$ - $E_2$ denotes the in-plane Young's modulus and $G_{ij}$ , $\nu_{ij}$ *(i,j=1,2,3)* for in-plane shear modulus and poisson ratio at $(\xi_1,\xi_2,\xi_3)$ axis respectively.

## Appendix-B. Definitions of $[K_{ij}]$ in Eq. (14(a))

$$K_{11} = A_{11}\frac{\partial^2}{\partial\xi_1^2} + A_{66}\frac{\partial^2}{\partial\xi_2^2} \tag{B.1}$$

$$K_{12} = \left(A_{12} + A_{66}\right)\frac{\partial^2}{\partial\xi_1\partial\xi_2} \tag{B.2}$$

$$K_{13} = \left(\frac{A_{11}}{\mp R_1} + \frac{A_{12}}{\mp R_2}\right)\frac{\partial}{\partial\xi_1} - c_1E_{11}\frac{\partial^3}{\partial\xi_1^3} - (2c_1E_{66} + c_1E_{12})\frac{\partial^3}{\partial\xi_1\partial\xi_2^2} \tag{B.3}$$

$$K_{14} = \left(B_{11} - c_1E_{11}\right)\frac{\partial^2}{\partial\xi_1^2} + \left(B_{66} - c_1E_{66}\right)\frac{\partial^2}{\partial\xi_2^2} \tag{B.4}$$

$$K_{15} = \left(B_{12} - c_1E_{12} + B_{66} - c_1E_{66}\right)\frac{\partial^2}{\partial\xi_1\partial\xi_2} \tag{B.5}$$

$$K_{22} = A_{66}\frac{\partial^2}{\partial\xi_1^2} + A_{22}\frac{\partial^2}{\partial\xi_2^2} \tag{B.6}$$

$$K_{23} = \left(\frac{A_{12}}{\mp R_1} + \frac{A_{22}}{\mp R_2}\right)\frac{\partial}{\partial\xi_2} - c_1E_{22}\frac{\partial^3}{\partial\xi_2^3} - (2c_1E_{66} + c_1E_{12})\frac{\partial^3}{\partial\xi_1^2\partial\xi_2} \tag{B.7}$$

$$K_{24} = \left(B_{12} - c_1E_{12} + B_{66} - c_1E_{66}\right)\frac{\partial^2}{\partial\xi_1\partial\xi_2} \tag{B.8}$$

$$K_{25} = \left(B_{66} - c_1E_{66}\right)\frac{\partial^2}{\partial\xi_1^2} + \left(B_{22} - c_1E_{22}\right)\frac{\partial^2}{\partial\xi_2^2} \tag{B.9}$$

$$\begin{aligned} K_{33} = {} & \left[A_{55} - 6c_1D_{55} + 9c_1^2F_{55} + c_1\left(\frac{E_{12}}{\mp R_1} + \frac{E_{22}}{\mp R_2}\right) + c_1\left(\frac{E_{11}}{\mp R_1} + \frac{E_{12}}{\mp R_2}\right)\right]\frac{\partial^2}{\partial\xi_1^2} \\ & + \left[A_{44} - 6c_1D_{44} + 9c_1^2F_{44} + 2c_1\left(\frac{E_{12}}{\mp R_1} + \frac{E_{22}}{\mp R_2}\right)\right]\frac{\partial^2}{\partial\xi_2^2} \\ & - 9c_1^2H_{11}\frac{\partial^4}{\partial\xi_1^4} - 2c_1^2(H_{12} + 2H_{66})\frac{\partial^4}{\partial\xi_1^2\partial\xi_2^2} \\ & - c_1^2H_{22}\frac{\partial^4}{\partial\xi_2^4} - \left[\left(\frac{A_{11}}{\mp R_1^2} + \frac{A_{12}}{\mp R_1(\mp R_2)}\right) + \left(\frac{A_{12}}{\mp R_1(\mp R_2)} + \frac{A_{22}}{\mp R_2^2}\right)\right] \end{aligned} \tag{B.10}$$

$$\begin{aligned} K_{34} = {} & \left[A_{55} - 6c_1D_{55} + 9c_1^2F_{55} - \frac{1}{\mp R_1}\left(B_{11} - c_1E_{11}\right) - \frac{1}{\mp R_2}\left(B_{12} - c_1E_{12}\right)\right]\frac{\partial}{\partial\xi_1} \\ & + c_1\left(F_{11} - c_1H_{11}\right)\frac{\partial^3}{\partial\xi_1^3} + \left[c_1\left(F_{12} - c_1H_{12}\right) + 2c_1\left(F_{66} - c_1H_{66}\right)\right]\frac{\partial^3}{\partial\xi_1\partial\xi_2^2} \end{aligned} \tag{B.11}$$

$$\begin{aligned} K_{35} = {} & \left[A_{44} - 6c_1D_{44} + 9c_1^2F_{44} - \frac{1}{\mp R_1}\left(B_{12} - c_1E_{12}\right) - \frac{1}{\mp R_2}\left(B_{22} - c_1E_{22}\right)\right]\frac{\partial}{\partial\xi_2} \\ & + c_1\left(F_{22} - c_1H_{22}\right)\frac{\partial^3}{\partial\xi_2^3} + \left[c_1\left(F_{12} - c_1H_{12}\right) + 2c_1\left(F_{66} - c_1H_{66}\right)\right]\frac{\partial^3}{\partial\xi_1^2\partial\xi_2} \end{aligned} \tag{B.12}$$

$$\begin{aligned} K_{44} = {} & \left[D_{11} - 2c_1F_{11} + c_1^2H_{11}\right]\frac{\partial^2}{\partial\xi_1^2} + \left[D_{66} - 2c_1F_{66} + c_1^2H_{66}\right]\frac{\partial^2}{\partial\xi_2^2} \\ & - \left(A_{55} + 6c_1D_{55} + 9c_1^2F_{55}\right) \end{aligned} \tag{B.13}$$

$$K_{45} = \left[D_{12} - c_1F_{12} + D_{66} - c_1F_{66} - c_1\left(F_{12} - c_1H_{12}\right) - c_1\left(F_{66} - c_1H_{66}\right)\right]\frac{\partial^2}{\partial\xi_1\partial\xi_2} \tag{B.14}$$

$$\begin{aligned} K_{55} = {} & \left[D_{66} - 2c_1F_{66} + c_1^2H_{66}\right]\frac{\partial^2}{\partial\xi_1^2} + \left[D_{22} - 2c_1F_{22} + c_1^2H_{22}\right]\frac{\partial^2}{\partial\xi_2^2} \\ & - A_{44} + 3c_1D_{44} + 3c_1\left(D_{44} - 3c_1F_{44}\right) \end{aligned} \tag{B.15}$$

where

$$c_1 = -\frac{4}{3h^2} \tag{B.16}$$